

## Supplementary Online Content

Palmqvist S, Zetterberg H, Blennow K, et al. Accuracy of brain amyloid detection in clinical practice using cerebrospinal fluid  $\beta$ -amyloid 42: a cross-validation study against amyloid positron emission tomography. *JAMA Neurol*. Published online August 25, 2014. doi:10.1001/jamaneurol.2014.1358.

**eAppendix 1.** Methods

**eAppendix 2.** Results and Discussion

**eFigure 1.** ROC Curves of the Accuracy of CSF Tau, P-tau, A $\beta$ 42/Tau or A $\beta$ 42/P-tau to Predict an Abnormal  $^{18}$ F-flutemetamol Scan (SUVR >1.42) in the Original Cohort

**eFigure 2.** Scatterplots of the SUVR Values for  $^{18}$ F-flutemetamol and CSF Tau (A), CSF P-tau (B), CSF A $\beta$ 42/Tau (C), and CSF A $\beta$ 42/P-tau (D) in the Original Cohort

**eReferences**

This supplementary material has been provided by the authors to give readers additional information about their work.

## eAppendix 1. Methods

### CSF collection and analysis

The CSF samples were collected into polypropylene tubes at the memory clinics in Malmö, Lund and Ängelholm over two years (2011-2013) according to routine clinical procedures, and the procedure and the analysis followed the Alzheimer's Association Flow Chart for lumbar puncture.<sup>1</sup> After centrifugation, the CSF samples obtained were frozen at -80°C and shipped to the Clinical Neurochemistry Laboratory in Mölndal, Sweden, on dry ice once a week for direct analyses. The CSF was analyzed continuously as part of routine clinical practice and consequently the CSF samples were analyzed sample by sample and not in batches. The personnel analyzing the CSF samples were not aware that the samples were part of a research study (and thus blinded to the amyloid PET results) and the obtained values were recorded in the patients' medical records as part of routine clinical practice. The samples were analyzed using commercially available enzyme-linked immunosorbent assays (ELISAs) (Innogenetics, Ghent, Belgium) to determine the levels of total tau, A $\beta$ 42 and tau phosphorylated at Thr181 (P-tau) (INNOTEST<sup>®</sup> hTAU Ag,  $\beta$ -AMYLOID<sub>(1-42)</sub> and PHOSPHO-TAU<sub>(181P)</sub>, respectively). All analyses were performed by board-certified laboratory technicians using procedures accredited by the Swedish Board for Accreditation and Conformity Assessment (SWEDAC). Longitudinal stability in the measurements over the study period was ascertained using an elaborate system of internal quality control samples and achieved through careful standardization of the protocols, testing of incoming kit lots and selection of those that bridged well with previous lots (see Table 1 in the main article and the eResult section for further details).

### <sup>18</sup>F-flutemetamol PET scanning

<sup>18</sup>F-flutemetamol is chemically similar to <sup>11</sup>C-Pittsburgh Compound B (PiB) except for the presence of an <sup>18</sup>F instead of an <sup>11</sup>C isotope.<sup>2</sup> The standardized uptake value ratios (SUVRs) of <sup>18</sup>F-flutemetamol correlate highly with <sup>11</sup>C-PiB ( $r = 0.89 - 0.92$ ) and the test-retest variability of regional SUVRs is 1–4%.<sup>3</sup> <sup>18</sup>F-flutemetamol was manufactured at the radiopharmaceutical production site in Risø, Denmark, using a FASTlab synthesizer module (GE Healthcare). Subjects received a single dose of <sup>18</sup>F-flutemetamol according to a method described previously.<sup>4</sup> PET/CT scanning of the whole brain was conducted at two sites (Malmö and Lund) using the same type of scanner, a Philips Gemini TF 16. The dynamic PET acquisition (6 frames, 5 min/frame) in 3D mode was started 90 min post-injection (p.i.) and was immediately followed by a low-dose (120 kVp, 80 mA) CT scan for attenuation correction. The PET images were reconstructed using the line-of-response row-action maximum-likelihood algorithm (LOR-RAMLA). The PET scans were always done after lumbar puncture and the median time interval between the lumbar puncture and PET imaging was 6.6 months (25th / 75th percentile; 3.7 / 9.9 months) in the original cohort. During such a time period no apparent changes are seen in the amyloid PET and CSF biomarkers.<sup>5-7</sup>

### <sup>18</sup>F-flutemetamol PET image processing and analysis

The analysis of <sup>18</sup>F-flutemetamol PET images were done at GE Healthcare, Life Sciences, Uppsala, Sweden, and the personnel at GE Healthcare had not access to any diagnostic information (including CSF biomarker levels) of the research subjects. Summed PET images from approximately 90–120 min p.i. were generated representing the average uptake of <sup>18</sup>F-flutemetamol over this time. The PET summed images were then spatially normalized into Montreal Neurologic Institute (MNI) standard space using a PET-only adaptive template registration method.<sup>8</sup> Magnetic resonance imaging (MRI) data were not used because they have not been shown to improve the quantification of <sup>18</sup>F-flutemetamol data.<sup>8</sup> The quality of the PET-only spatial normalization was assessed by manually comparing it with an MRI T1 template from the International Consortium for Brain Mapping (ICBM), resampled to the image matrix dimension of the PET image. All PET images were accurately spatially normalized. A volume of interest (VOI) template<sup>8</sup> defined in MNI space for a range of cortical and subcortical regions was applied to sample activity in bilateral prefrontal, parietal, lateral temporal, sensorimotor, occipital, and mesial temporal cortices, the anterior cingulate, posterior cingulate and precuneus (the two latter measured as the same region), as well as the pons and cerebellar cortex. This template uses relatively narrow VOIs to minimize white matter contamination. A neocortical composite region (VOI) was defined as previously described.<sup>8</sup> The correct positioning of the VOIs for whole-brain, pons and cerebellar cortex relative the PET image was confirmed. The SUVR was defined as the regional tracer uptake in a VOI normalized for the mean uptake in a reference region, which in this case was the cerebellar cortex because it is notably free of fibrillar plaques. PET images were classified as 'normal' or 'abnormal' based on the SUVR of the composite VOI.

### **Measures of hippocampus atrophy and cognition**

All patients were examined using a single 3T MR scanner (Trio, Siemens, Erlangen, Germany). The images were automatically processed with FreeSurfer version 5.1 (<http://surfer.nmr.mgh.harvard.edu>) to extract regional volumetric measurements and afterwards visually inspected to ensure that the correct region had been assessed. Measures of the left and right hippocampal volumes were compared and the smaller of the two volumes was used in the analyses. Global cognition was rated with the MMSE. Episodic memory was assessed using the Rey Auditory Verbal Learning Test (RAVLT).<sup>9</sup> The raw score from the immediate recall of five oral presentations of 15 nouns was used.

### **Statistical analysis**

The composite (see above) SUVR of <sup>18</sup>F-flutemetamol was used for all analyses, except for the correlation analyses of the regional SUVR data. An unbiased cutoff value for an abnormal <sup>18</sup>F-flutemetamol scan was established using a mixture model, which determines the cutoff in an independent way. Mixture modeling is a 2-step procedure based on an expectation maximization algorithm, which assumes that the <sup>18</sup>F-flutemetamol data are a mixed sample from two different normal distributions (in this case one with a normal A $\beta$  deposition and one with an abnormal A $\beta$  deposition). Different initial conditions were used in 100 iterated calculations and they all resulted in the same cutoff. The method has been described in more detail previously.<sup>10</sup> Differences between the cohorts (Table 1) were analyzed with either Mann-Whitney (continuous variables) or the X<sup>2</sup> test (dichotomous variables). Sensitivity and specificity was calculated using receiver operating characteristics (ROC) analysis and the cutoff was optimized at the highest Youden index (sensitivity + specificity - 1). Logistic regression analysis was used to calculate odds ratios and when adjusting for other factors in the dichotomized calculations of CSF A $\beta$ 42 levels and SUVRs of <sup>18</sup>F-flutemetamol. Both backward and forward likelihood ratio (LR) methods were used with identical results. <sup>18</sup>F-flutemetamol was set as the dependent variable (dichotomized at SUVR 1.42) and CSF A $\beta$ 42 (dichotomized at  $\leq 647$  pg/mL), age, sex, *APOE* (presence of one or two  $\epsilon 4$  alleles), RAVLT, MMSE and education were entered as covariates/independent variables. Spearman correlation was used to examine linear relations (e.g. correlations with regional A $\beta$  deposition). All analyzes were performed in the original cohort. The validation cohort was only used to test the CSF A $\beta$ 42 threshold established in the original cohort. A *P* value of less than 0.05 was considered to indicate statistical significance. Otherwise, a 95% confidence interval (CI) was specified. Mixture modeling was performed with R version 3.0 (R Foundation for Statistical Computing, Vienna, Austria, 2013), ROC analyses with MedCalc version 11.5 (MedCalc Software, Mariakerke, Belgium) and all other analyses with SPSS (IBM release 2011, version 20.0; IBM SPSS Statistics for Mac. Armonk, NY).

## **eAppendix 2. Results and Discussion**

### **CSF quality control**

Two internal control samples (aliquots of pooled Alzheimer-like and control-like CSF) were analyzed on each ELISA plate, for quality control (QC) purposes. For T-tau, the coefficient of variation (CV) was 9.6% for the Alzheimer QC sample (n= 236; mean 907 pg/mL) and 7.1% for the control QC sample (n= 230; mean 288 pg/mL). For P-tau, the CV was 9.4% for the Alzheimer QC sample (n= 195; mean 105 pg/mL) and 9.1% for the control QC sample (n= 187; mean 44 pg/mL). For CSF A $\beta$ 42, the CV was 10.2% for the Alzheimer QC sample (n= 331; mean 449 pg/mL) during the first part of the study, and 11.4% for a new QC sample (n= 110; mean 460 pg/mL) during the second part of the study, while the CV was 11.5% for the control QC sample (n= 440; mean 667 pg/mL).

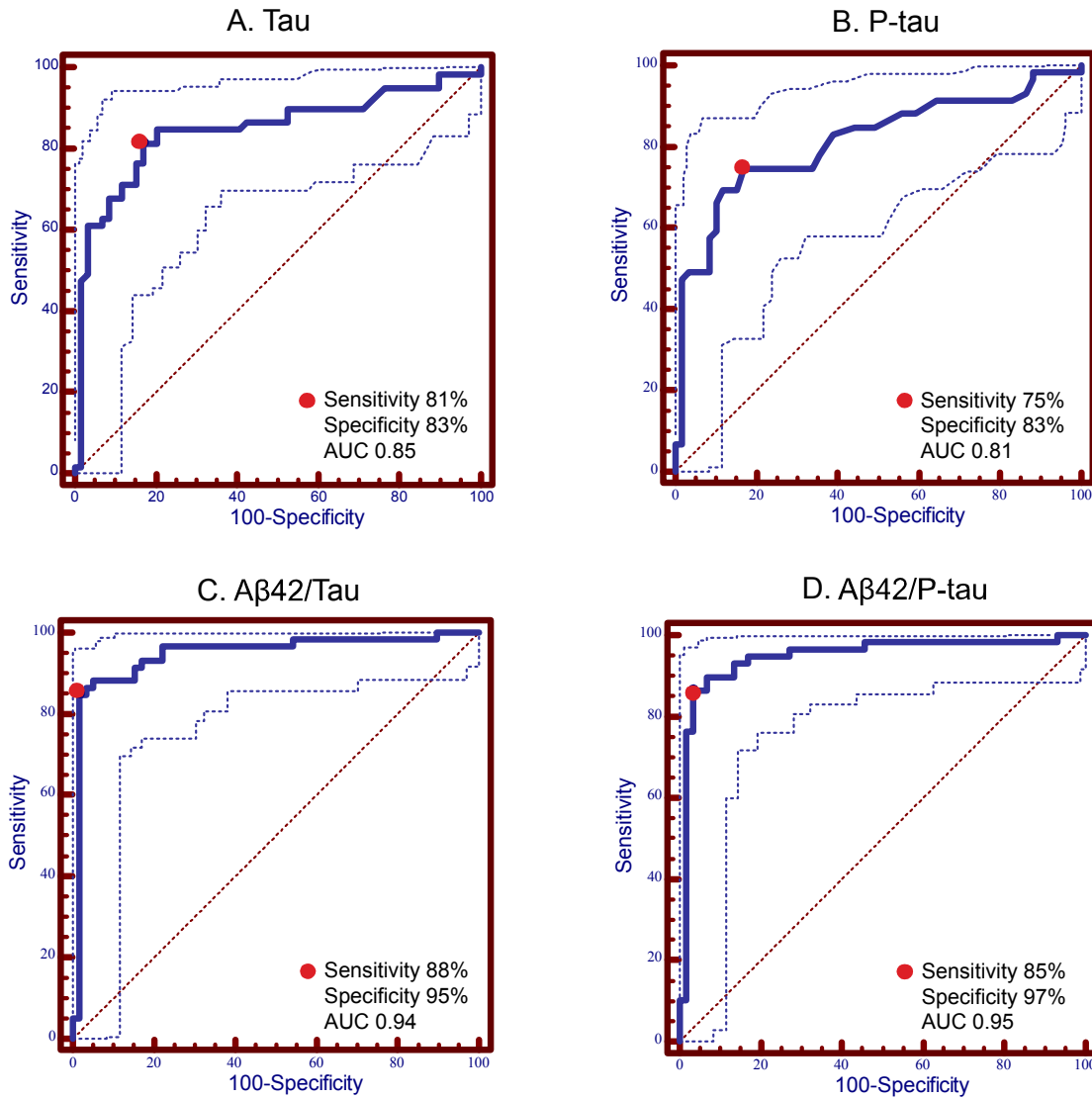
### **Agreement between CSF A $\beta$ 42 and amyloid PET in patients with subjective cognitive complaints vs mild cognitive impairment**

The accuracy of CSF A $\beta$ 42 for distinguishing an abnormal amyloid PET from a normal amyloid PET was compared among patients with MCI and those with subjective cognitive symptoms in the entire population ("original cohort" and "validation cohort", n = 156). The AUC was 0.93 (95% CI 0.85–0.98) among patients with MCI (n = 77). Among those with subjective symptoms (n = 79), the AUC was almost identical (0.94, 95% CI 0.86-0.98). Hence, no relevant difference in CSF A $\beta$ 42 accuracy was found between patients with subjective and objective cognitive symptoms.

### **Discordant CSF A $\beta$ 42 and <sup>18</sup>F-flutemetamol results**

In our study, there were discordant results between CSF A $\beta$ 42 and <sup>18</sup>F-flutemetamol in a few cases, similar to other studies.<sup>11, 12</sup> Two patients (one borderline) with abnormal amyloid scans had normal CSF A $\beta$ 42 and five patients (one borderline) with abnormal CSF A $\beta$ 42 had normal PET scans in the original cohort (Figure 2B). In the validation cohort, there were only two discordant results (Figure 2D). A reason for the discordant results could be that CSF detects soluble A $\beta$  while the SUVR of amyloid PET corresponds to neuritic plaques/fibrillar A $\beta$ .<sup>13, 14</sup> Two studies have argued that the cases with A $\beta$ 42+/PET- could be the result of decreased A $\beta$ 42 before the increase of fibrillar amyloid deposition on PET scans.<sup>13, 15</sup> However, a recent study suggested that A $\beta$ 42-/PET+ was much more common in earlier disease stages than A $\beta$ 42+/PET-, which instead supports the assumption that amyloid PET becomes abnormal first.<sup>12</sup> Whether these discordant results are caused by different properties of the modalities, reflect a certain stage in the progression of AD or are caused by a specific phenotype within the disease spectrum of AD remains to be tested in longitudinal studies with repeated clinical assessments, CSF samplings and amyloid PET scans. Yet another cause of discordant results is the AD-causing Arctic *APP* mutation that causes pre-fibrillar (not fibrillar) A $\beta$  deposition and hence an A $\beta$ 42+/PET- result.<sup>16</sup> Finally, a limitation of the present study was the time interval between lumbar puncture and PET imaging, which could result in false positive cases with discordant A $\beta$ 42-/PET+ results, because PET imaging was always done after lumbar puncture. However, the cases with A $\beta$ 42-/PET+ were very few in the present study (2% of total cases) and when excluding all cases with a time period exceeding 6 months between lumbar puncture and PET imaging the results were virtually unchanged (agreement between CSF A $\beta$ 42 and <sup>18</sup>F-flutemetamol was then 94%;  $\kappa=0.88$ ).

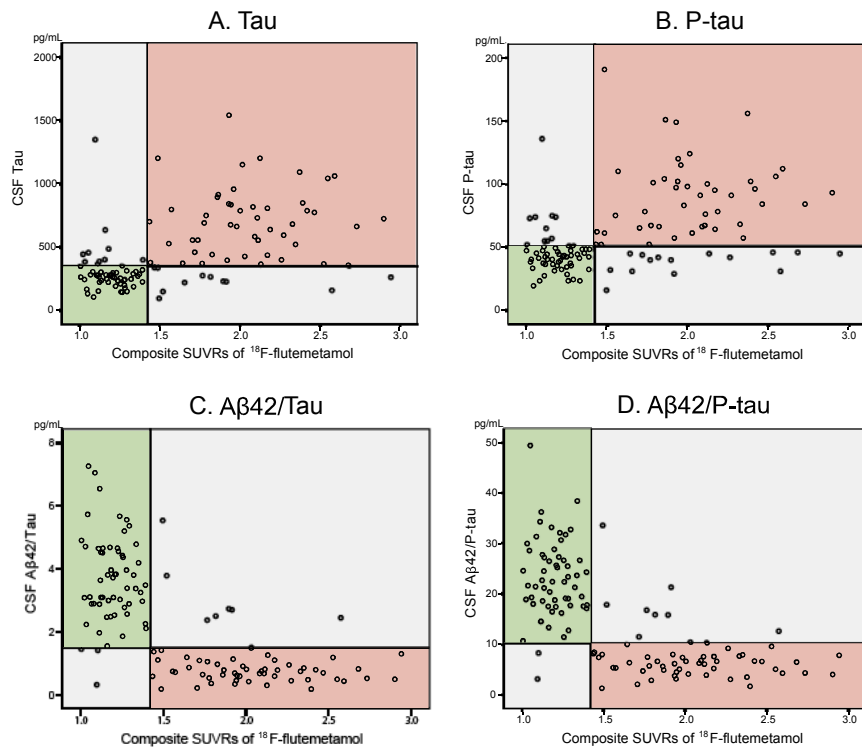
# eFigure 1



**eFigure 1.** ROC Curves of the Accuracy of CSF Tau, P-tau, Aβ42/Tau or Aβ42/P-tau to Predict an Abnormal <sup>18</sup>F-flutemetamol Scan (SUVR >1.42) in the Original Cohort

The dashed lines represent the 95% CI and the red dot the optimal cutoff. Panel A, CSF Tau (AUC 0.85, 95% CI 0.77–0.91, optimal cutoff >350 pg/mL). Panel B, CSF P-tau (AUC 0.81, 95% CI 0.73–0.88, optimal cutoff >51 pg/mL). Panel C, CSF Aβ42/Tau (AUC 0.94, 95% CI 0.89–0.98, optimal cutoff ≤1.5). Panel D, CSF Aβ42/P-tau (AUC 0.95, 95% CI 0.89–0.98, optimal cutoff ≤10.3).

eFigure 2



**eFigure 2.** Scatterplots of the SUVR Values for  $^{18}\text{F}$ -flutemetamol and CSF Tau (A), CSF P-tau (B), CSF A $\beta$ 42/Tau (C), and CSF A $\beta$ 42/P-tau (D) in the Original Cohort. The vertical lines represent the cutoff for an abnormal  $^{18}\text{F}$ -flutemetamol scan (SUVR >1.42) and the horizontal lines represent the optimal CSF cutoffs derived from the ROC analysis (eFigure 1) to predict an abnormal  $^{18}\text{F}$ -flutemetamol scan.

## eReferences

1. Blennow K, Hampel H, Weiner M, Zetterberg H. Cerebrospinal fluid and plasma biomarkers in Alzheimer disease. *Nat Rev Neurol*. 2010;6(3):131-144.
2. Klunk WE, Engler H, Nordberg A, Wang Y, Blomqvist G, Holt DP, Bergstrom M, Savitcheva I, Huang GF, Estrada S, Ausen B, Debnath ML, Barletta J, Price JC, Sandell J, Lopresti BJ, Wall A, Koivisto P, Antoni G, Mathis CA, Langstrom B. Imaging brain amyloid in Alzheimer's disease with Pittsburgh Compound-B. *Ann Neurol*. 2004;55(3):306-319.
3. Vandenberghe R, Van Laere K, Ivanoiu A, Salmon E, Bastin C, Triau E, Hasselbalch S, Law I, Andersen A, Korner A, Minthon L, Garraux G, Nelissen N, Bormans G, Buckley C, Owenius R, Thurfjell L, Farrar G, Brooks DJ.  $^{18}\text{F}$ -flutemetamol amyloid imaging in Alzheimer disease and mild cognitive impairment: a phase 2 trial. *Ann Neurol*. 2010;68(3):319-329.
4. Koole M, Lewis DM, Buckley C, Nelissen N, Vandenbulcke M, Brooks DJ, Vandenberghe R, Van Laere K. Whole-body biodistribution and radiation dosimetry of  $^{18}\text{F}$ -GE067: a radioligand for in vivo brain amyloid imaging. *J Nucl Med*. 2009;50(5):818-822.
5. Buchhave P, Blennow K, Zetterberg H, Stomrud E, Londos E, Andreasen N, Minthon L, Hansson O. Longitudinal study of CSF biomarkers in patients with Alzheimer's disease. *PLoS One*. 2009;4(7):e6294.
6. Mattsson N, Portelius E, Rolstad S, Gustavsson M, Andreasson U, Stridsberg M, Wallin A, Blennow K, Zetterberg H. Longitudinal cerebrospinal fluid biomarkers over four years in mild cognitive impairment. *J Alzheimers Dis*. 2012;30(4):767-778.

7. Villemagne VL, Burnham S, Bourgeat P, Brown B, Ellis KA, Salvado O, Szoëke C, Macaulay SL, Martins R, Maruff P, Ames D, Rowe CC, Masters CL. Amyloid beta deposition, neurodegeneration, and cognitive decline in sporadic Alzheimer's disease: a prospective cohort study. *Lancet Neurol.* 2013;12(4):357-367.
8. Lundqvist R, Lilja J, Thomas BA, Lotjonen J, Villemagne VL, Rowe CC, Thurfjell L. Implementation and validation of an adaptive template registration method for 18F-flutemetamol imaging data. *J Nucl Med.* 2013;54(8):1472-1478.
9. Strauss E, Sherman E, Spreen O. *A Compendium of Neuropsychological Tests 3ed*: Oxford University Press Inc.; 2006.
10. Benaglia T, Chauveau D, Hunter DR, Young D. mixtools: An R Package for Analyzing Finite Mixture Models. *ournal of Statistical Software.* 2009;32(6):1-29.
11. Koivunen J, Pirttila T, Kempainen N, Aalto S, Herukka SK, Jauhianen AM, Hanninen T, Hallikainen M, Nagren K, Rinne JO, Soininen H. PET amyloid ligand [11C]PIB uptake and cerebrospinal fluid beta-amyloid in mild cognitive impairment. *Dement Geriatr Cogn Disord.* 2008;26(4):378-383.
12. Landau SM, Lu M, Joshi AD, Pontecorvo M, Mintun MA, Trojanowski JQ, Shaw LM, Jagust WJ. Comparing PET imaging and CSF measurements of Ass. *Ann Neurol.* 2013.
13. Fagan AM, Mintun MA, Shah AR, Aldea P, Roe CM, Mach RH, Marcus D, Morris JC, Holtzman DM. Cerebrospinal fluid tau and ptau(181) increase with cortical amyloid deposition in cognitively normal individuals: implications for future clinical trials of Alzheimer's disease. *EMBO Mol Med.* 2009;1(8-9):371-380.
14. Ni R, Gillberg PG, Bergfors A, Marutle A, Nordberg A. Amyloid tracers detect multiple binding sites in Alzheimer's disease brain tissue. *Brain.* 2013;136(Pt 7):2217-2227.
15. Morris JC, Roe CM, Xiong C, Fagan AM, Goate AM, Holtzman DM, Mintun MA. APOE predicts amyloid-beta but not tau Alzheimer pathology in cognitively normal aging. *Ann Neurol.* 2010;67(1):122-131.
16. Scholl M, Wall A, Thordardottir S, Ferreira D, Bogdanovic N, Langstrom B, Almkvist O, Graff C, Nordberg A. Low PiB PET retention in presence of pathologic CSF biomarkers in Arctic APP mutation carriers. *Neurology.* 2012;79(3):229-236.